JCI The Journal of Clinical Investigation

13C-nuclear magnetic resonance spectroscopy studies of hepatic glucose metabolism in normal subjects and subjects with insulin-dependent diabetes mellitus.

G W Cline, … , L D Katz, G I Shulman

J Clin Invest. 1994;94(6):2369-2376. https://doi.org/10.1172/JCI117602.

Research Article

To determine the effect of insulin-dependent diabetes mellitus (IDDM) on rates and pathways of hepatic glycogen synthesis, as well as flux through hepatic pyruvate dehydrogenase, we used 13C-nuclear magnetic resonance spectroscopy to monitor the peak intensity of the C1 resonance of the glucosyl units of hepatic glycogen, in combination with acetaminophen to sample the hepatic UDP-glucose pool and phenylacetate to sample the hepatic glutamine pool, during a hyperglycemic-hyperinsulinemic clamp using [1-13C]-glucose. Five subjects with poorly controlled IDDM and six age-weight-matched control subjects were clamped at a mean plasma glucose concentration of approximately 9 mM and mean plasma insulin concentrations approximately 400 pM for 5 h. Rates of hepatic glycogen synthesis were similar in both groups (approximately 0.43 +/- 0.09 mumol/ml liver min). However, flux through the indirect pathway of glycogen synthesis (3 carbon units-->-->glycogen) was increased by approximately 50% ($P < 0.05$), whereas the relative contribution of pyruvate oxidation to TCA cycle flux was decreased by approximately 30% ($P < 0.05$) in the IDDM subjects compared to the control subjects. These studies demonstrate that patients with poorly controlled insulin-dependent diabetes mellitus have augmented hepatic gluconeogenesis and relative decreased rates of hepatic pyruvate oxidation. These abnormalities are not immediately reversed by normalizing intraportal concentrations of glucose, insulin, and glucagon and may contribute to postprandial hyperglycemia.

^{13}C-Nuclear Magnetic Resonance Spectroscopy Studies of Hepatic Glucose Metabolism in Normal Subjects and Subjects with Insulin-dependent Diabetes Mellitus

Gary W. Cline, Douglas L. Rothman, Inger Magnusson, Lee D. Katz, and Gerald I. Shulman
Departments of Internal Medicine and Diagnostic Radiology, Yale University School of Medicine, New Haven, Connecticut 06520-8020

Abstract

To determine the effect of insulin-dependent diabetes mellitus (IDDM) on rates and pathways of hepatic glycogen synthesis, as well as flux through hepatic pyruvate dehydrogenase, we used ^{13}C-nuclear magnetic resonance spectroscopy to monitor the peak intensity of the C1 resonance of the glucosyl units of hepatic glycogen, in combination with acetaminophen to sample the hepatic UDP-glucose pool and phenylacetate to sample the hepatic glutamine pool, during a hyperglycemic–hyperinsulinemic clamp using [1-^{13}C]-glucose. Five subjects with poorly controlled IDDM and six age-weight-matched control subjects were clamped at a mean plasma glucose concentration of ~ 9 mM and mean plasma insulin concentrations ~ 400 pM for 5 h. Rates of hepatic glycogen synthesis were similar in both groups (~ 0.43±0.09 μmol/ml liver · min). However, flux through the indirect pathway of glycogen synthesis (3 carbon units →→ glycogen) was increased by ~ 50% ($P < 0.05$), whereas the relative contribution of pyruvate oxidation to TCA cycle flux was decreased by ~ 30% ($P < 0.05$) in the IDDM subjects compared to the control subjects. These studies demonstrate that patients with poorly controlled insulin-dependent diabetes mellitus have augmented hepatic gluconeogenesis and relative decreased rates of hepatic pyruvate oxidation. These abnormalities are not immediately reversed by normalizing intraportal concentrations of glucose, insulin, and glucagon and may contribute to postprandial hyperglycemia. (*J. Clin. Invest.* 1994. 94:2369–2376.)
Key words: glycogen • gluconeogenesis • NMR spectroscopy • pyruvate dehydrogenase

Introduction

After a glucose load, liver glycogen is synthesized by both direct (glucose → glucose-6-phosphate → glucose-1-phosphate → UDP-glucose → glycogen), and indirect (3 carbon units →→ phosphoenolpyruvate →→ glucose-6-phosphate → glucose-1-phosphate → UDP-glucose → glycogen) pathways (1–4). Animal studies have shown that fluxes through these pathways are regulated by substrate and hormonal concentrations (4–6) as well as by diet (2, 7). In a recent study in humans we have shown that the percent flux through the direct pathway is dependent on the dietary state, such that ~ 50% of the glycogen is derived directly from glucose after an overnight fast, and that the direct pathway increases to ~ 70% following breakfast (2). It might be anticipated that liver glycogen metabolism would be altered in patients with poorly controlled type I or insulin-dependent diabetes mellitus (IDDM)[1] in response to chronically altered concentrations of glucose, insulin, and glucagon.

The goals of this study were to assess the impact of poorly controlled IDDM on: (*a*) the rates of hepatic glycogen synthesis, (*b*) the relative contributions of the direct and indirect pathways to hepatic glycogen synthesis, and (*c*) the relative intrahepatic flux of pyruvate dehydrogenase (PDH) to tricarboxylic acid (TCA) cycle flux. Rates of liver glycogen synthesis were measured in subjects with poorly controlled IDDM and in age-weight-matched control subjects under identical conditions of portal vein hyperglycemia–hyperinsulinemia–hypoglucagonemia using ^{13}C-nuclear magnetic resonance spectroscopy (NMR) in conjunction with the glucose–insulin clamp technique (8). In order to determine the relative fluxes through the direct pathway of hepatic glycogen synthesis and the relative flux through PDH/TCA, the glucose infusate was enriched with [1-^{13}C]glucose and hepatic pools of UDP-glucose and glutamine were noninvasively sampled by oral administration of acetaminophen and phenylacetate, respectively (1, 2, 9). The percent of hepatic glycogen synthesized by the direct pathway was determined by comparison of isotopic enrichment of plasma glucose with that of plasma and urine acetaminophen-glucuronide (1, 2). The flux of pyruvate oxidation relative to the TCA cycle flux was estimated from analysis of the ^{13}C enrichment in the individual carbons of the glutamyl moiety of liver conjugated phenylacetyl-glutamine (9).

Methods

Subjects. Five subjects with insulin-dependent diabetes mellitus (four men and one woman) and six healthy normal control subjects (four men and two women) were studied. All subjects were within 5% of their ideal body weight according to the 1959 Metropolitan Life Insurance tables. The mean (±SE) weight in the diabetic and control subjects was 72.8±2.3 kg and 66.7±1.5 kg, respectively; their mean ages were 32±3 and 29±2 yr. Subjects with IDDM had a mean glycosylated hemoglobin of 14.1±1.7% (normal range 4–8%). No subject had any major disease other than diabetes mellitus or was taking medications other than insulin. None of the control subjects had a family history of diabetes.

Address correspondence to Dr. Gerald I. Shulman, Department of Internal Medicine, Fitkin 1, 333 Cedar Street, New Haven, CT 06520-8020
Received for publication 2 June 1994 and in revised form 2 August 1994.

J. Clin. Invest.

0021-9738/94/12/2369/08 $2.00
Volume 94, December 1994, 2369–2376

1. *Abbreviations used in this paper:* APE, atom percent excess; GC-MS, gas chromatography-mass spectroscopy; IDDM, insulin-dependent diabetes mellitus; ISIS, image selected in vivo spectroscopy; MRI, magnetic resonance imaging; NMR, nuclear magnetic resonance spectoscopy; PDH, pyruvate dehydrogenase; PEPCK, phospo-enol-pyruvate carboxykinase; TCA, tricarboxylic acid.

Informed consent was obtained from all subjects after the purpose, nature, and potential risks of the study were explained to them. The protocol was reviewed and approved by the Human Investigation Committee of the Yale University School of Medicine.

Experimental protocol. All studies were begun at 8 a.m. after an overnight fast of 12–14 h. 3 d before the study, all subjects were given a weight-maintaining diet (prepared by the metabolic kitchen of the Yale New Haven Hospital General Clinical Research Center) of 33 g/kg body wt consisting of 50% carbohydrate, 20% protein, and 30% fat. On the afternoon before the study, all subjects were admitted to the Yale New Haven Hospital General Clinical Research Center, given a liquid meal similar in content to the dinners on the previous days. After the meal the volume of the liver was measured with magnetic-resonance imaging (MRI). In order to induce normoglycemia, all diabetic subjects received an overnight variable infusion of insulin (0.6–1.5 pmol per kg of body wt per min) through a Teflon catheter placed in an antecubital vein. The induction of euglycemia allowed the diabetic and normal subjects to be studied while they had the same plasma glucose concentrations and in response to an identical increment above baseline in the plasma glucose concentration. On the morning of the study a second Teflon catheter was inserted into the antecubital vein of the opposite arm to permit blood to be drawn. Intravenous catheters were inserted in each arm of the normal subjects on the morning of the study.

Hyperglycemic–hyperinsulinemic clamp procedure. Hyperglycemia–hyperinsulinemia was induced with the insulin–glucose clamp technique (8). To inhibit endogenous insulin and glucagon secretion, an infusion of somatostatin (0.1 μg/kg body wt per min) was initiated 5 min before the start of the glucose–insulin infusion in both the normal and diabetic subjects. At time = 0 min, insulin (Humulin-R; Eli Lilly, Indianapolis, IN) was administered in a priming and continuous infusion of 240 pmol per square meter of body surface area per min to raise the plasma insulin concentration acutely and maintain it at ~ 400 pmol/liter for 5 h. At the same time, a variable priming infusion of [1-^{13}C]glucose (1.11 M, 10–99% enriched) was begun so that the plasma glucose concentration could be raised acutely and maintained at ~ 9 mM for 180 min. At this time the infusate was switched to natural abundance [^{13}C] glucose (1.11 M) for the duration of the study. At the start of the glucose–insulin clamp, 1.5 g of acetaminophen and 1.0 g of phenylacetate were administered orally.

Plasma glucose concentration was measured every 5 min throughout the study and the infusion rate of the glucose solution was periodically adjusted to maintain the desired hyperglycemic plateau. Blood samples for determination of insulin, glucagon, C peptide, and lactate concentrations as well as ^{13}C enrichment in glucose and acetaminophen–glucuronide were taken every 15 min. Urine samples for ^{13}C-acetaminophen-glucuronide and ^{13}C-phenylacetyl-glutamine were collected at hourly intervals throughout the clamp. Under these conditions of constant hyperglycemia and hyperinsulinemia, hepatic glucose production is completely suppressed and all infused glucose is taken up by tissue, except for a minor amount excreted in urine. The latter amount was quantitated, and the rate of excretion was subtracted from the rate of glucose infusion. Therefore, the mean glucose infusion rate, minus urinary glucose excretion, served as a measure of the total amount of glucose metabolized.

Magnetic-resonance imaging. Clinical imaging of all patients was performed on a 1.5 T magnet (General Electric Co., Milwaukee, WI). Multiecho axial scanning was performed (TE20/80, TR2000) as previously described (10). Accuracy of the measurement was assessed with water-filled phantoms of known volume and determined to be ±5% with a coefficient of variation of ±1%.

In vivo NMR spectroscopic techniques. In order to assess rates of hepatic glycogen synthesis ^{13}C-NMR spectra were obtained over an ~ 70-min interval during the second hour of the hyperglycemic–hyperinsulinemic clamp. These measurements were limited to this period of time in order to minimize subject discomfort from having to lie motionless in the magnet the entire time. ^{13}C-NMR signals were obtained with a 9-cm circular ^{13}C observation coil and a 12-cm coplanar butterfly ^{1}H-decoupler coil placed rigidly over the lateral aspect of the liver in the supine subject, as previously described (10). Briefly, we determined initial coil placement by percussing the borders of the liver. The magnet was shimmed with the water signal obtained from the decoupling coil. The position of the coil over the liver was confirmed by imaging the liver from the surface coil with a multislice gradient echo image. Localized ^{13}C-NMR liver spectra were obtained with a modified one dimensional image selected in vivo spectroscopy (ISIS) localization technique to remove signals from the surface above the liver (11). A 4-ms hyperbolic secant pulse was used to invert the 2.5 cm of the skin surface, and as a result signals from the surface were eliminated by adding scans with an alternate inversion pulse. A 180° pulse at the coil center was used as an excitation pulse and it was calibrated each time using a 2-cm sphere containing ^{13}C-enriched formic acid which was placed at coil center. Each proton-decoupled ^{13}C-NMR spectrum consisted of 6,400 scans which were acquired for 15 min. All spectra were processed and analyzed in an identical fashion. Hepatic glycogen was quantified by integration of the C1 glycogen peak at 100.5 ppm with a Bruker Aspect 3000 computer using the same frequency bandwidth for all spectra (250 Hz). Absolute quantitation of hepatic glycogen was determined by comparing the peak integral of the C1 liver glycogen peak with the C1 glycogen peak integral of a glycogen standard taken under identical conditions. Finally, minor corrections (< 10%) were made for incomplete space filling of the surface coil by the liver by comparison of the axial images of the glycogen phantom with that of the subject's liver.

Indirect calorimetry. Continuous indirect calorimetry was performed before the hyperglycemic clamp and for 20 min every hour during the hyperglycemic clamp as previously described (12).

Analytical procedures. Plasma glucose concentration was measured by the glucose oxidase method (Glucose Analyzer II; Beckman Instrs., Inc., Fullerton, CA). Plasma immunoreactive free insulin, C peptide, and glucagon were measured with double antibody radio-immunoassay techniques using commercially available kits (insulin; Diagnostic Sys. Labs., Inc., Webster, TX; C peptide, Diagnostic Products Corp., Los Angeles, CA; and glucagon, ICN Biomedicals Inc., Irvine, CA). Glycosylated hemoglobin was measured using an ion exchange chromatography method (Isolab, Inc., Akron, OH). ^{13}C atom percent enrichment (APE) of plasma glucose, amino acids, and acetaminophen-glucuronide were determined by GC-MS following suitable derivatization. Plasma glucose was derivatized as the pentaacetate, following $Ba(OH)_2/ZnSO_4$ deproteinization and purification by anion/cation exchange chromatography (AG1-X8, AG50W-X8; Bio Rad Laboratories, Richmond, CA), as previously described (2). Plasma acetaminophen-glucuronide was derivatized by a modification of that used for amino acids (13). Plasma was deproteinized with $Ba(OH)_2/ZnSO_4$, the supernatant freeze-dried, and C6 of the glucuronide moiety esterified with acidified *n*-butanol:3 N HCl (100°C for 1 h), the residual *n*-butanol was evaporated under a stream of dry nitrogen. The glucuronide *n*-butyl ester was acylated with acetic anhydride:pyridine (60°C for 30 min). Isotopic enrichment of urine acetaminophen-glucuronide and phenylacetyl-glutamine were determined by NMR and GC-MS. Acetaminophen-glucuronide and phenylacetyl-glutamine in urine were purified by anion exchange chromatography (AG1-X8, 100–200 mesh, acetate form), as previously described (2). The purified acetaminophen-glucuronide and phenylacetyl-glutamine were dissolved in 0.4 ml of D_2O for NMR analysis of ^{13}C isotopic enrichment. Following NMR analysis, an aliquot (50 μl) was dried, the glucuronide derivatized, as described above, and analyzed by GC-MS.

Gas chromatography-mass spectroscopy. GC-MS analysis was performed with an Hewlett-Packard 5890 gas chromatograph (HP-1 capillary column, 12 m × 0.2 mm × 0.33 μm film thickness) interfaced to a Hewlett-Packard 5971A Mass Selective Detector operating in the positive chemical ionization mode with methane as reagent gas. For glucose-pentaacetate and acetaminophen-glucuronide (*n*-butyl ester, triacetate), GC conditions were isothermal at 200°C. Selected ion monitoring was used to determine enrichment in various molecular ion fragments. Ions with m/z 331, 332, and 333 were monitored for glucose C1 → C6 APE. For acetaminophen-glucuronide, ions with m/z 198/197 were monitored for determination of isotopic enrichment in C1 → C5, and m/z 299/300 and 359/360 for enrichment in C1 → C6.

Analytical NMR spectroscopy. ^{13}C isotopic enrichment of the glutamyl moiety of phenyacetyl-glutamine, and of the glucuronide moiety of

acetaminophen-glucuronide were determined by ^{13}C-NMR spectroscopy performed on a Bruker 500 MHz spectrometer (Bruker Instruments, Inc., Billerica, MA). Unlabeled carbons in the phenylacetyl and acetaminophen moieties served as internal standards in the determination of ^{13}C isotopic abundance of the glutamyl or glucuronide moieties. Isotopic abundance was determined from comparison of the peak areas of the carbons within each conjugate. In order to minimize correction factors used to compensate for differences in nOe and relaxation times between carbons, comparison of NMR peak areas were limited to carbons of similar hybridization or NMR chemical shift. A delay of 6.0 s between scans and an 30° pulse width was used to acquire all spectra obtained in this study. Correction factors ranged from 0.96 (glutamyl C1 vs phenylacetyl C1) to 1.06 (glutamyl C3 and C4 vs phenylacetyl C2).

^{13}C-NMR chemical shifts of acetaminophen-glucuronide and phenylacetyl-glutamine were assigned from pure standards and mixtures, after taking into account the expected change in the ^{13}C chemical shift due to conjugation of phenylacetate with glutamine, and acetaminophen with glucuronic acid. Chemical shifts were referenced to trimethylsilylpropionate-(2, 2, 3, 3-d_4) assigned to 0 ppm. (MSD Isotopes Div., Montreal, Canada). The ^{13}C-NMR chemical shifts of glucuronide C1, C2, and C6 were assigned to 101.0, 73.2, and 176.1 ppm, respectively. In the acetaminophen moiety, C2′ (C6′) and C3′ (C5′) of the aromatic ring were assigned to 117.7 and 123.8 ppm (chemical shifts not specified). For the glutamyl moiety of phenylacetyl-glutamine, we assigned the ^{13}C-NMR chemical shift for C1 as 176.0 ppm, C2 as 53.3 ppm, C3 as 27.3 ppm, C4 as 32.1 ppm, and C5 as 178.8 ppm. For the phenylacetyl moiety of phenylacetyl-glutamine, we assigned the ^{13}C-NMR chemical shift for C1 as 175.7 ppm and C2 as 43.0 ppm. The chemical shift assignment of C1 of the phenylacetyl moiety was confirmed from the spectra of synthetic phenylacetylglutamine enriched with ^{13}C in the carbonyl C of the phenyacetyl moiety.

HPLC. HPLC analysis of plasma acetaminophen-glucuronide concentration was performed with an Hewlett-Packard 1090 liquid chromatograph (HP ODS Hypersil column, 5.0 μ, 100 × 4.6 mm; 45°C) equipped with a Filter Photometric Detector (254 nm). A binary solvent system (flow rate 0.75 ml/min) of sodium acetate (0.45 M in water, pH adjusted to 4.15 with phosphoric acid) and acetonitrile (isocratic for 3 min, 92% aqueous: 8% acetonitrile, followed by a linear increase to 20% acetonitrile in 2 min, with this concentration held constant for 3 min) was used to achieve resolution of acetaminophen-glucuronide. Standard acetaminophen-glucuronide was the gift of McNeil Pharmaceuticals (Fort Washington, PA).

Calculations. The rate of glycogen synthesis was calculated from the increase in ^{13}C glycogen concentration during the [1-^{13}C]glucose infusion. The increase in total (^{13}C + ^{12}C) liver glycogen concentration (Δ[Gly]) was calculated for each chosen time interval (in the present study 15-min intervals were used) by the following equation:

$$\Delta[\text{Gly}] = [\Delta\text{PI}\cdot a\cdot 100]/[(\text{APE } glc\cdot b) + 1.1] \quad (1)$$

where PI = peak intensity, a = ^{13}C glycogen concentration per intensity unit (mmol/liter liver), APE glc = atom percent excess ^{13}C over baseline in plasma glucose, and b = dilution factor. The dilution factor (b) represents the fraction of UDP-glucose formed from the direct pathway as determined from the ^{13}C APE in C1 and C6 of plasma glc and acetaminophen-glucuronide from the following equation:

$$\%\ \text{Direct Pathway (b)} = [(\text{C1 APE} - \text{C6 APE})\ \textit{glucuronide}]/[(\text{C1 APE} - \text{C6 APE})\ \textit{glc}] \quad (2)$$

The net rate of glycogen synthesis is the slope of the line in a plot of the increase in total glycogen concentration versus time, as determined from the best fit of the data to a line calculated by method of least squares. The equations for estimation of V_{PDH}/V_{TCA}, $V_{FUM}/(V_{TCA} + V_{PEPCK})$ and $(V_{PEPCK} + V_{TCA})/V_{TCA}$ are derived in the Appendix.

The results are expressed as means±standard error of the means. Comparisons between groups were made by the unpaired Student *t* test, and within groups with analysis of variance with Student–Newman–Keuls post hoc testing.

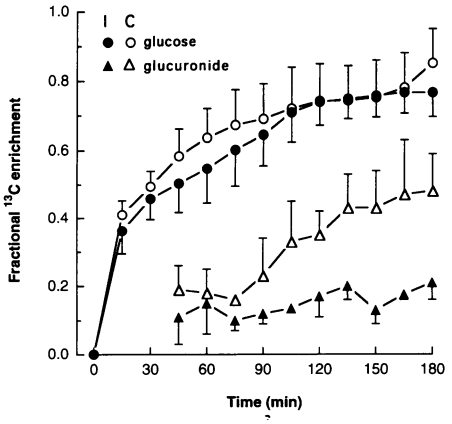

Figure 1. Plasma ^{13}C glucose enrichment (normalized to infusate ^{13}C glucose enrichment) in control subjects (C, *open circles*) and subjects with IDDM (I, *solid circles*), and plasma ^{13}C-acetaminophen-glucuronide enrichment (normalized to infusate ^{13}C glucose enrichment) in control subjects (*open triangles*) and subjects with IDDM (*solid triangles*) before and during the hyperglycemic–hyperinsulinemic clamp study. Values are means±SE.

Results

Hyperglycemic–hyperinsulinemic clamp. Fasting plasma glucose and free insulin concentrations were slightly higher in the IDDM subjects (6.6±0.5 mM and 82±6 pM) compared to the control subjects (5.2±0.2 mM and 58±7 pM), however, once the hyperglycemic clamp was started the mean steady-state plasma glucose concentration (control, 8.7±0.1 mM; IDDM, 9.1±0.1 mM) and free insulin concentration (controls, 411±12 pM; IDDM, 402±24 pM) were similar in the two groups. Before the start of the hyperglycemic clamp the mean plasma glucagon concentration was slightly higher in the IDDM subjects than the control subjects (control, 58±8 pg/ml; IDDM, 82±6 pg/ml). Once the hyperglycemic clamp was started the mean plasma glucagon concentrations became similar between the two groups (control, 55±8 pg/ml; IDDM, 56±4 pg/ml). There was no difference in basal blood lactate concentration between the two groups (controls, 0.65±0.07 μM; IDDM, 0.59±0.04 μM), but mean steady-state blood lactate concentration was less in the IDDM subjects compared to the controls, 0.91±0.04 and 1.27±0.13 μM, respectively ($P < 0.05$). Fig. 1 shows the ^{13}C isotopic enrichment of plasma glucose and acetaminophen-glucuronide (normalized to the ^{13}C isotopic enrichment of the infusate) in both groups. During the last hour of the ^{13}C-glucose infusion, the ^{13}C enrichment of plasma glucose changed by less than 7% and the ^{13}C-acetaminophen-glucuronide enrichment changed by less than 3% in both groups. Whole body glucose metabolism increased significantly with time in both groups, 6.26±0.93 versus 11.19±1.14 mg/kg body wt·min from 60–120 min and 10.31±1.11 vs 17.20±2.03 mg/kg body wt·min from 180–240 min, but was consistently less in the IDDM subjects compared to the control subjects, respectively ($P < 0.05$). Mean rates of oxidative glucose metabolism were similar between the two groups (controls, 4.14±0.54 mg/kg body wt·min; IDDM, 3.60±0.36 mg/kg body wt·min) and did not change during the clamp.

Pathways of liver glycogen synthesis. ^{13}C enrichments in both plasma acetaminophen-glucuronide and urinary acetaminophen-glucuronide were examined. Because of the time it takes for the plasma acetaminophen-glucuronide to be excreted in the urine, the enrichment of plasma acetaminophen-glucuronide more closely represents that of intrahepatic acetaminophen-glucuronide and UDP-glucose in time than does the acetaminophen-glucuronide collected in the urine. Urine glucuronide provides an integrated enrichment over a longer time period, and can be used as a check on enrichments obtained from plasma glucuronide. In all cases there was excellent agreement (±9%) between the two measurements. The ^{13}C enrichment of plasma acetaminophen-glucuronide was significantly less in the IDDM than in the control subjects throughout the study (Fig. 1). The percentage of glycogen synthesized by the direct pathway was calculated from the ratio of enrichment in C1 (minus C6) of glucuronide to plasma glucose (1, 2). For this calculation it was necessary to estimate the time between acetaminophen conjugation in the liver, appearance in plasma and excretion in urine. This was directly assessed in each experiment by comparing the time it took the ^{13}C enrichment in plasma and urinary acetaminophen-glucuronide to decrease relative to the time it took for the ^{13}C plasma glucose enrichment to decrease during the unlabeled glucose infusion which was begun at $t \sim 180$ min. The lag time for plasma ^{13}C-glucuronide was ~ 30 min and for urinary glucuronide was ~ 45 min. These values agree well with a previous study (14). It should be emphasized that the lag time has very little effect on our calculated values of the percent direct pathway. We found values of 30–90 min in the lag time gave less than 4% variance in the percent direct flux calculated for glucuronide collected during the chase period. This method also assumes that acetaminophen is hepatically conjugated to glucuronide and excreted at a similar rate for both IDDM and control subjects. This assumption was directly verified by measuring urinary acetaminophen-glucuronide excretion rates (~ 1.5 mg/min in both IDDM and control subjects) as well as the time it took for plasma acetaminophen-glucuronide concentration to reach a maximum concentration (~ 30 min in both IDDM and control subjects) which were similar in both groups. The percent direct flux of glucose into hepatic glycogen was about half that in the IDDM subjects compared to control subjects throughout the study as determined by both the ^{13}C enrichments in plasma acetaminophen-glucuronide relative to that in plasma glucose (Fig. 1) as well as by the ^{13}C enrichments in urinary acetaminophen-glucuronide relative to that in plasma glucose (Fig. 2).

Hepatic glycogen synthesis. The rate of [1-^{13}C]glucose incorporation into C1 glycogen was linear in both groups (IDDM subjects, $r = 0.9985$; control subjects, $r = 0.9998$) and the rates of hepatic glycogen synthesis were calculated to be 0.49±0.10 μmol/ml liver · min in the control group and 0.46±0.07 in the IDDM group. Liver volumes were found to be similar in both groups (controls, 1.5±0.1 liters; IDDM, 1.5±0.1 liters). Hepatic glycogen synthesis, including both direct and indirect pathways, was found to account for 18±4% and 26±3% ($P < 0.05$) of nonoxidative glucose metabolism in the control and IDDM subjects, respectively. The rates of hepatic glycogen synthesis from the direct pathway of hepatic glycogen synthesis were calculated to be 0.15±0.02 and 0.28±0.06 μmol/ml liver · min, accounting for 9±1% and 11±3% of nonoxidative glucose metabolism in the IDDM and control subjects, respectively.

PDH/TCA flux. During the course of this study, the TCA cycle intermediates became enriched in ^{13}C from glycolysis of

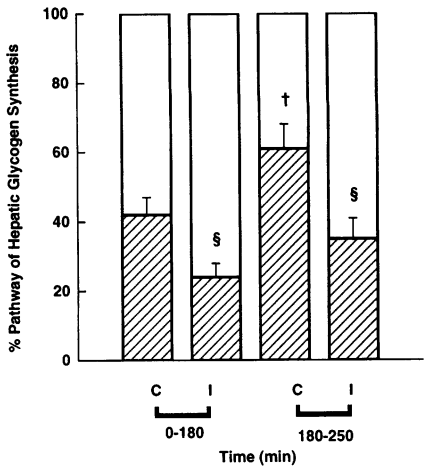

Figure 2. Percent direct (*hatched bars*) and indirect (*open bars*) pathways of liver glycogen synthesis in the control (C) and IDDM (I) subjects during the hyperglycemic–hyperinsulinemic clamp study. Values are means±SE. $^{\S}P < 0.05$ compared to controls. $^{\dagger}P < 0.05$ compared to initial time for controls.

[1-^{13}C]glucose. We used phenylacetate to determine the isotopic labeling pattern of intrahepatic α-ketoglutarate (9). Phenylacetate is conjugated with hepatic glutamine which is derived from hepatic α-ketoglutarate. The absolute enrichment of any of the TCA cycle intermediates is dependent on the enrichment of pyruvate and on flux into the TCA cycle of other carbon sources. Although label in phenylacetyl-glutamine may be diluted in comparison to α-ketoglutarate from equilibration with a pool of unlabeled glutamine, equilibration of glutamine with α-ketoglutarate should not appreciably change the relative distribution of ^{13}C within the molecule. Therefore, analysis of the relative ^{13}C distribution of intrahepatic glutamine (as phenylacetyl-glutamine) will be representative of intrahepatic α-ketoglutarate.

Table I lists the ^{13}C atom percent enrichments in the carbons of the glutamyl moiety (designated G1, G2, G3, G4, and G5) of urinary phenylacetyl-glutamine. The enrichments are tabulated only for those carbon positions and time points in which the enrichment exceeded 0.15% which was our lower limit of sensitivity. As shown the intramolecular ^{13}C enrichments of phenylacetyl-glutamine; G3/G2, G4/(G2 + G3), and (G2+G5)/G1 remained relatively constant during the last 220 min of the study in both groups. Equilibration of oxaloacetate with fumarate (FUM) is calculated from the ratio of G3 to G2, complete equilibration being equal to 1 (9). As observed previously in normal subjects (9), equilibration is not complete, and it appears that IDDM does not affect the extent of equilibration since in both cases the G3 to G2 ratio is ~ 0.8. The ratio of G4 to (G2 + G3) is an index of the flux of pyruvate which enters the TCA cycle by decarboxylation to acetyl-CoA followed by condensation with oxaloacetate to form succinate. Acetyl-CoA which is hydrolyzed to acetate or which is used for ketone body or fatty acid synthesis is not included in this ratio (9). As can be seen in the table, the mean relative flux of pyruvate oxidation relative to TCA cycle flux was ~ 30% less ($P < 0.05$) in the diabetic subjects compared to the control subjects at all time points.

Discussion

In this study we examined the effect of poorly controlled insulin-dependent diabetes mellitus on hepatic glucose metabolism using ^{13}C-nuclear magnetic resonance spectroscopy to monitor the peak intensity of the C1 resonance of the glucosyl units of

Table I. Distribution of ^{13}C in the Carbons of the Glutamine Moiety of Urinary Phenylacetylglutamine Excreted by Subjects Given [1-^{13}C]Glucose

Subject	Urine collection	^{13}C Atom percent enrichment					G3/G2	G4/(G2 + G3)	(G2 + G5)/G1
		G1	G2	G3	G4	G5			
	h								
Controls									
J.P.	1.5–2.5	0.60	0.91	0.63	1.00	0.17	0.69	0.65	1.80
	2.5–3.5	0.82	1.70	1.24	2.31	0.20	0.73	0.79	2.32
	3.5–4.2	0.54	1.81	1.54	2.82		0.85	0.84	3.35
H.L.	2.0–3.0		0.30	0.25	0.25		0.83	0.45	
	3.0–4.0	0.16	0.47	0.34	0.57		0.72	0.70	2.94
	4.0–5.0	0.23	0.92	0.76	1.05		0.83	0.63	4.00
	5.0–6.0	0.26	1.00	0.82	1.23		0.82	0.68	3.85
I.M.	1.5–3.0		0.24	0.21	0.38		0.88	0.84	
	3.0–4.0		0.58	0.47	0.63		0.81	0.60	
	4.0–5.0		0.58	0.52	1.16		0.90	1.05	
	5.0–6.5	0.31	0.68	0.46	1.05		0.68	0.92	2.19
S.C.	2.0–3.0	0.2	0.38	0.26	0.45		0.68	0.70	1.90
	3.0–4.0	0.28	0.83	0.57	0.96		0.69	0.69	2.96
K.M.	2.5–4.0		0.36	0.28	0.41		0.78	0.64	
	4.0–5.0		0.58	0.51	0.70		0.88	0.64	
	5.0–6.0		0.49	0.45	0.67		0.92	0.71	
M.K.	3.0–4.0		0.38	0.32	0.48		0.84	0.69	
	4.0–5.5		0.62	0.48	0.73		0.77	0.66	
					†Mean of control subjects		0.79	0.71	2.68
						SEM	0.02	0.03	0.31
IDDM									
F.S.	0–2.5		0.32	0.27	0.37		0.84	0.63	
	2.5–4.0		0.66	0.59	0.76		0.89	0.61	
	4.0–4.5	0.33	1.25	1.09	1.46		0.87	0.62	3.79
	4.5–5.5	0.99	2.17	1.83	2.53	0.21	0.84	0.63	2.40
	5.5–6.5	1.13	2.51	2.20	3.28	0.15	0.88	0.70	2.35
J.K.	3.5–4.5		0.74	0.52	0.67		0.70	0.53	
	4.5–5.5	0.15	1.08	1.09	1.17		1.01	0.54	7.20
	5.5–6.5	0.17	1.05	0.82	1.01		0.78	0.54	6.18
W.W.	2.5–4.5		0.40	0.35	0.27		0.88	0.36	
	4.5–6.0	0.33	0.85	0.63	0.53	0.15	0.74	0.36	3.03
	5.0–6.0	0.23	0.87	0.69	0.62		0.79	0.40	3.78
	6.0–7.0	0.39	0.98	0.83	0.87		0.85	0.48	2.51
B.J.	2.0–3.5		0.32	0.30	0.29		0.94	0.47	
	3.5–4.5		0.51	0.43	0.46		0.84	0.49	
	4.5–6.5	0.17	0.66	0.52	0.57		0.79	0.48	3.88
M.J.	2.5–4.0		0.21	0.17	0.17		0.81	0.45	
	4.0–6		0.24	0.26	0.30		1.08	0.60	
					†Mean of IDDM subjects		0.86	0.52	4.13
						SEM	0.02	0.04	0.88

† Mean of the individual means.

hepatic glycogen, in combination with acetaminophen to sample the hepatic UDP-glucose pool and phenylacetate to sample the hepatic glutamine pool, during a hyperglycemic–hyperinsulinemic clamp using [1-^{13}C]glucose. Whole body glucose metabolism was significantly less in the IDDM subjects compared with the control subjects, however there was no significant difference in the mean rates of hepatic glycogen synthesis between the two groups. From the linear increase in the intensity of the [1-^{13}C]glycogen peak, rates of hepatic glycogen synthesis were calculated to be 0.46±0.07 and 0.49±0.10 μmol/ml liver · min,

accounting for 26±3% and 18±4% of nonoxidative glucose metabolism in the IDDM and control subjects, respectively. To the extent that liver glycogen turnover is occurring, these rates will overestimate net hepatic glycogen synthetic rates. Although estimates of liver glycogen turnover in IDDM subjects are currently not available, we have estimated glycogen turnover to be 31±8% of the glycogen synthetic rate (0.43±0.09 μmol/ml liver · min) in normal subjects studied under similar conditions (15). Using this value the rate of net hepatic glycogen synthesis might be estimated to be ~ 0.34 μmol/g liver · min in the control subjects. This value is in excellent agreement with a previous study in which the rate of net hepatic glycogen synthesis was estimated to be 0.32 μmol/g liver · min as determined from two liver biopsy samples in a similar group of young healthy subjects studied under similar conditions (16).

In a recent study we examined hepatic glycogen synthesis in IDDM and normal subjects during the course of a day in which three mixed meals were ingested. In contrast to the present results, we found that the IDDM subjects, who were taking their daily insulin in their usual fashion and were in fair glycemic control (mean glycosylated hemoglobin 10.2±0.3%, normal range 4–8%), had a profound defect in net hepatic glycogen synthesis such that by the end of the day they had synthesized only one third the amount of hepatic glycogen that was synthesized by the normal control subjects (17). Furthermore, compared to the control subjects, a much larger proportion of their hepatic glycogen was synthesized by the indirect (gluconeogenic) pathway. Taken together these studies suggest that alterations in portal vein concentrations of insulin and glucagon contribute to the abnormalities in net hepatic glycogen synthesis observed in IDDM subjects eating mixed meals, since matching portal vein concentrations of insulin and glucagon in the present study was able to normalize rates of hepatic glycogen synthesis. In contrast, matching portal vein concentrations of glucose, insulin, and glucagon did not normalize the relative fluxes of hepatic glycogen synthesis in that the indirect pathway was found to be proportionately about twice as active in the IDDM subjects compared to the control subjects throughout the study. These results are also in accord with animal studies by Giaccari et al. (18) who studied normal and partially pancreatectomized Sprague–Dawley rats during a hyperglycemic–hyperinsulinemic clamp and found no differences in net hepatic glycogen synthetic rates, but a significant increase in the indirect pathway.

Increased rates of gluconeogenesis have important clinical implications for patients with IDDM. Normal glucose tolerance following a meal depends on suppression of hepatic glucose production (19). Since hepatic glycogenolysis has been shown in dogs to be more sensitive to inhibition by insulin than gluconeogenesis, the increased activity of hepatic gluconeogenesis observed in the IDDM subjects might be expected to contribute to postprandial hyperglycemia (20). These results also suggest that the chronic alterations in the hormonal and/or substrate milieu associated with poorly controlled IDDM results in augmentation of the gluconeogenic pathway that is not immediately reversible by normalization of intraportal concentrations of insulin and glucagon.

In addition to tracing the pathways of hepatic glycogen synthesis with acetaminophen we also traced the flux of pyruvate into the TCA cycle using phenylacetate as previously described (9). Phenylacetate is a naturally occurring compound that can be taken in gram quantities by humans. Once ingested it is conjugated to glutamine in the liver and excreted in the urine (9). Assuming that most of the excreted ^{13}C-labeled phenylacetyl-glutamine is synthesized from intrahepatic α-ketoglutarate via glutamate, the labeling of phenylacetyl-glutamine collected in the urine can be used to reflect the ^{13}C-labeling in the hepatic α-ketoglutarate pool (9). An estimate of pyruvate dehydrogenase flux into the TCA cycle can be obtained by the ^{13}C-labeling in the carbon 4 position of glutamine (G4) relative to the enrichments in the carbon 2 and carbon 3 positions (G2, G3) of glutamine (Appendix, Eq. 3). This relationship assumes that flux through pyruvate carboxylase is the major flux into the oxaloacetate pool. A recent study has shown that pyruvate carboxylase flux is at least three times greater than the TCA cycle flux in overnight fasted humans under similar conditions (9). As shown in the table the relative flux through pyruvate dehydrogenase into the TCA cycle was decreased by ~ 30% in the IDDM subjects compared to the control subjects. This suggests that the livers of poorly controlled IDDM individuals are relatively more dependent on fat oxidation as an energy source for metabolism compared to nondiabetic individuals. This observation is consistent with pyruvate dehydrogenase in-

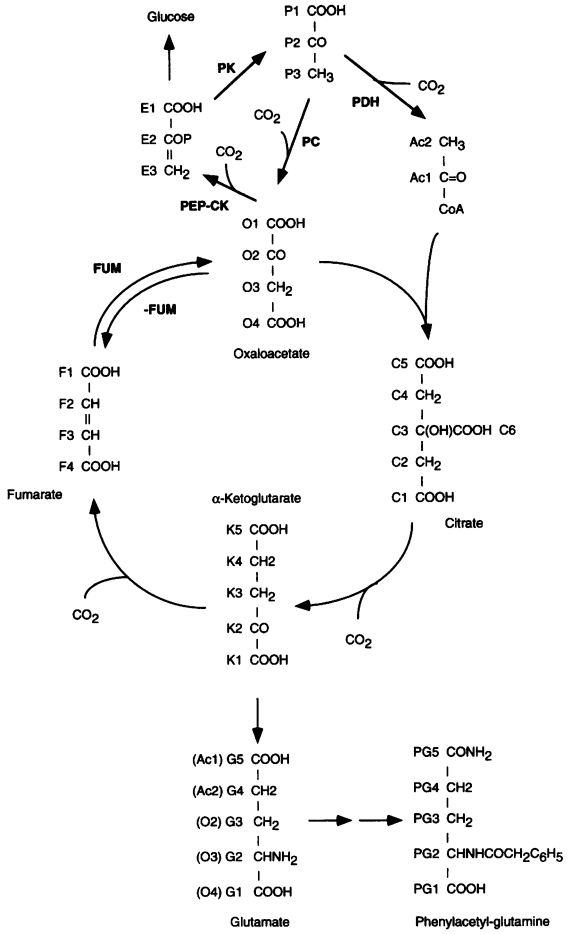

Figure 3. Steady state model of TCA cycle and gluconeogenesis. The carbon atoms are designated: Ac (acetate), C (citrate), E (phospho-enol-pyruvate), F (fumarate), G (glutamate), K (α-ketoglutarate), O (oxaloacetate), P (pyruvate), and PG (phenylacetyl-glutamine), the superscript 13 denotes ^{13}C atom percent enrichment at the designated molecular position. Abbreviations used are: PK (pyruvate kinase), PDH (pyruvate dehydrogenase), PC (pyruvate carboxylase), PEPCK (phospho-enol pyruvate carboxykinase), FUM (fumarase in the forward direction) and -FUM (fumarase in the reverse direction). V denotes flux mediated by those enzymes.

hibition by acetyl-CoA and NADH formed during fatty acid oxidation and the higher rates of gluconeogenesis observed in the IDDM subjects.

Equilibration between oxaloacetate, malate, and fumarate was also estimated by the relative ^{13}C-labeling between C2 and C3 glutamine. If there was complete equilibration between these metabolites the amount of ^{13}C-labeling in C2 glutamine should equal the ^{13}C-labeling in C3 glutamine. We found that equilibration between these metabolites was almost but not totally complete in that the ratio of C3 glutamine to C2 glutamine was ~ 80% in both normal and IDDM subjects, which is similar to what has previously been observed in healthy subjects after an overnight fast using ^{14}C lactate as a precursor (9). From these data it can be estimated that the relative flux through fumarase is about 10 times greater than the combined flux through phosphoenolpyruvate carboxykinase and the TCA cycle (Appendix, Eq. 4).

An index of phospo-enol-pyruvate carboxykinase (PEPCK) to TCA cycle flux was also obtained from the ratio of enrichments in G2 + G5 to G1 of phenylacetyl-glutamine (Appendix, Eq. 5). This ratio provides an index of the relative flux via the indirect pathway independent of that provided by analysis of the enrichment in acetaminophen-glucuronide and plasma glucose. However, due to ^{13}C incorporation into C1 glutamate from $^{13}CO_2$ this provides a minimum estimate of the PEPCK flux relative to the TCA flux (Fig. 3). Based on a previous study in overnight fasted humans approximately half the ^{13}C enrichment in G1 was from $^{13}CO_2$ (9). An enhanced pyruvate carboxylase flux would lead to a greater underestimate of PEPCK/TCA. Although not statistically significant due to the low enrichment in G1 and the small sample size, the trend is towards greater PEPCK flux in the IDDM subjects compared to the control subjects. This observation is consistent with the higher flux through the indirect pathway that was observed in the IDDM subjects.

We conclude that patients with poorly controlled insulin-dependent diabetes mellitus have significant alterations in intrahepatic carbon flux such that the gluconeogenic pathway is augmented by ~ 50% and the relative contribution of pyruvate to TCA cycle oxidation is decreased by ~ 30%. These abnormalities are not immediately reversed by normalizing intraportal concentrations of glucose, insulin, and glucagon and may contribute to postprandial hyperglycemia in patients with insulin dependent diabetes mellitus.

Appendix

Single pool steady state equations for: (refer to Table I and Fig. 3)

Derivation for V_{PDH}/V_{TCA} cycle flux in terms of C2, C3, and C4 glutamate:

$$\delta(^{13}O2 + {}^{13}O3)/\delta t = V_{TCA}(^{13}G4 + {}^{13}G3) + (^{13}P3 \times V_{PC}) - (^{13}O2 + {}^{13}O3)(V_{TCA} + V_{PEPCK})$$

at steady state: $\delta(^{13}O2 + {}^{13}O3)/\delta t = 0$

Therefore,

$$V_{TCA}(^{13}G4 + {}^{13}G3) + {}^{13}P3 \times V_{PC} = (^{13}O2 + {}^{13}O3)(V_{TCA} + V_{PEPCK})$$

but,

$$^{13}P3 = {}^{13}G4 \times V_{TCA}/V_{PDH} \text{ and } (^{13}O2 + {}^{13}O3) = (^{13}G2 + {}^{13}G3).$$

Substituting and solving in terms of enrichment ratios, we have,

$$^{13}G4/(^{13}G2 + {}^{13}G3) = (V_{PDH}/V_{TCA})\,[V_{TCA}(^{13}G2/(^{13}G2 + {}^{13}G3)) + V_{PC}]/[V_{PDH} + V_{PC}].$$

Under these experimental conditions,

$V_{PEPCK} \approx V_{PC}$ and $V_{PC} \geq 3 \times V_{TCA}$ and $V_{TCA} \geq V_{PDH}$ (reference 9).

Thus,

$$^{13}G4/(^{13}G2 + {}^{13}G3) \sim V_{PDH}/V_{TCA}. \quad (3)$$

Derivation for $V_{FUM}/(V_{PEPCK} + V_{TCA})$ flux in terms of C2 and C3 glutamate:

$$\delta\,^{13}O2/\delta t = 1/2V_{FUM}\,(^{13}O2 + {}^{13}O3) - {}^{13}O2(V_{-FUM} + V_{TCA} + V_{PEPCK}) \text{ at steady state: } \delta\,^{13}O2/\delta t = 0.$$

Therefore,

$$^{13}O2/(^{13}O2 + {}^{13}O3) = V_{FUM}/[2(V_{-FUM} + V_{TCA} + V_{PEPCK})].$$

Under these experimental conditions,

$V_{PEPCK} \approx V_{PC} \gg V_{TCA}$ and $V_{FUM} = V_{-FUM} + V_{TCA}$ (reference 9).

Therefore,

$$^{13}O2/(^{13}O2 + {}^{13}O3) \approx (V_{-FUM} + V_{TCA})/[2(V_{-FUM} + V_{TCA} + V_{PEPCK})].$$

Thus,

$$(^{13}O2 + {}^{13}O3)/{}^{13}O2 \approx 2[1 + V_{PEPCK}/(V_{-FUM} + V_{TCA})]$$

since $^{13}O2 = {}^{13}G2$ and $^{13}O3 = {}^{13}G3$

$$(1 + {}^{13}G3/{}^{13}G2) \approx 2[1 + V_{PEPCK}/(V_{-FUM} + V_{TCA})]. \quad (4)$$

Derivation for $(V_{PEPCK} + V_{TCA})/V_{TCA}$ cycle flux in terms of C1, C2, and C5 glutamate:

$$\delta\,^{13}O4/\delta t = V_{TCA}\,(^{13}A\,1/2 + {}^{13}O3/2) + V_{PC}(K\,{}^{13}CO_2 + (1 - K)\,{}^{13}P1) - {}^{13}O4(V_{TCA} + V_{PEPCK})$$

where $2K \approx {}^{13}G2/{}^{13}G3$

at steady state: $\delta\,^{13}O2/\delta t = 0$.

Therefore,

$$V_{TCA}\,(^{13}A\,1/2 + {}^{13}O3/2) + V_{PC}(K\,{}^{13}CO_2 + (1 - K)\,{}^{13}P1) = {}^{13}O4(V_{TCA} + V_{PEPCK})$$

but,

$^{13}O4 = {}^{13}G1$, $^{13}O3 = {}^{13}G2$, and $^{13}A1 = {}^{13}G5$.

Expressing in terms of glutamine enrichments, we have,

$$^{13}G1/(^{13}G2 + {}^{13}G5) = 1/2 \times V_{TCA}/(V_{TCA} + V_{PEPCK}) + [K{}^{13}CO_2 + (1 - K){}^{13}P1]/(^{13}G2 + {}^{13}G5) \times V_{PC}/(V_{TCA} + V_{PEPCK}).$$

If we assume,

$$(^{13}G2 + {}^{13}G5) \gg [K{}^{13}CO_2 + (1 - K){}^{13}P1].$$

Therefore,

$$(G2 + G5)/(G1) \sim 2 \times (V_{TCA} + V_{PEPCK})/V_{TCA}. \quad (5)$$

Acknowledgments

We are indebted to the nurses and staff of the Yale New Haven Hospital General Clinical Research Center, and Veronica Walton for technical assistance.

This work was supported by grants from the National Institutes of Health: DK-34576, DK-40936, DK-45735, RR-03475, M01-RR-00125-26, and a grant from the Juvenile Diabetes Foundation, Intl. (G. I. Shulman).

References

1. Magnusson, I., V. Chandramouli, W. C. Schumann, K. Kumaran, J. Wahren, and B. R. Landau. 1987. Quantitation of the pathways of hepatic glycogen formation on ingesting a glucose load. *J. Clin. Invest.* 80:1748–1754.

2. Shulman, G. I., G. Cline, W. C. Schumann, V. Chandramouli, K. Kumaran, and B. R. Landau. 1990. Quantitative comparison of pathways of hepatic glycogen repletion in fed and fasted humans. *Am. J. Physiol.* 259 (*Endocrinol. Metab. 22*):E335–E341.

3. Newgard, C. B., J. J. Hirsch, D. W. Foster, and J. D. McGarry. 1983. Studies on the mechanism by which exogenous glucose is converted into liver glycogen in the rat. *J. Biol. Chem.* 258:8046–8052.

4. Newgard, C. B., S. V. Moore, D. W. Foster, and J. D. McGarry. 1984. Efficient hepatic glycogen synthesis in refeeding rats requires continued carbon flow through the gluconeogenic pathway. *J. Biol. Chem.* 259:6058–6963.

5. Lang, C. H., G. J. Bagby, H. L. Blakeslye, J. L. Johnson, and J. J. Spitzer. 1986. Plasma glucose concentration determines direct versus indirect liver glycogen synthesis. *Am. J. Physiol.* 251 (*Endocrinol. Metab. 14*):E584–E590.

6. Shulman, G. I., R. A. DeFronzo, and L. Rossetti. 1991. Differential effect of hyperglycemia and hyperinsulinemia on pathways of hepatic glycogen repletion. *Am. J. Physiol.* 260 (*Endocrinol. Metab. 23*):E731–E735.

7. Rossetti, L., D. L. Rothman, R. A. DeFronzo, and G. I. Shulman. 1989. Effect of dietary protein on in vivo insulin action and liver glycogen repletion. *Am. J. Physiol.* 257 (*Endocrinol. Metab. 20*):E212–E219.

8. DeFronzo, R. A., J. E. Tobin, and R. Andres. 1979. Glucose clamp techniques: a method for quantifying insulin secretion and resistance. *Am. J. Physiol. 237* (*Endocrinol. Metab.*):E214–E223.

9. Magnusson, I., W. C. Shumann, G. E. Bartsch, V. Chandramouli, K. Kumaraan, J. Wahren, and B. R. Landau. 1991. Noninvasive tracing of Krebs cycle metabolism in liver. *J. Biol. Chem.* 266:6975–6984.

10. Rothman, D. L., I. Magnusson, L. D. Katz, R. G. Shulman, and G. I. Shulman. 1991. Quantitation of hepatic glycogenolysis and gluconeogenesis in fasting humans with ^{13}C NMR. *Science (Wash. DC)*. 254:573–576.

11. Ordidge, R. J., J. Connelly, and A. B. Lohman. 1986. Image-selected in vivo spectroscopy (ISIS): A new technique for spatially localized NMR spectroscopy. *J. Mag. Reson.* 66:283–294.

12. G. I. Shulman, D. L. Rothman, T. Jue, P. Stein, R. A. DeFronzo, and R. G. Shulman. 1990. Quantitation of muscle glycogen synthesis in normal subjects and subjects with non-insulin-dependent diabetes by ^{13}C nuclear magnetic resonance spectroscopy. *N. Engl. J. Med.* 322:223–228.

13. Leimer, K. R., R. H. Rice, and C. W. Gehrke. 1974. Amino acid analysis, hydrolysis, ion-exchange cleanup, derivatization, and quantitation by gas-liquid chromatography. *J. Chromatogr.* 94:113–133.

14. Hellerstein, M. K., D. J. Greenblatt, and H. N. Munro. 1987. Glyconjugates as noninvasive probes of intrahepatic metabolism: I. kinetics of label incorporation with evidence of a common precursor UDP-glucose pool for secreted glyconjugates. *Metabolism.* 36:988–994.

15. Magnusson, I., D. L. Rothman, B. Jucker, G. W. Cline, R. G. Shulman, and G. I. Shulman. 1994. Liver glycogen turnover in fed and fasted humans. *Am. J. Physiol.* 29:E796–E803.

16. Nilsson, L. H. Son, and E. Hultman. 1974. Liver and muscle glycogen in man after glucose and fructose infusion. *Scand. J. Clin. Lab. Invest.* 33:5–10.

17. Hwang, J. H., G. Perseghin, D. L. Rothman, G. Cline, I. Magnusson, K. Petersen, and G. I. Shulman. 1994. Alterations in hepatic glycogen synthesis in type I diabetes mellitus during a defined mixed meal diet. *Diabetes.* 43(Suppl. 1) 73A, #238.

18. Giaccari, A., and L. Rossetti. 1992. Predominant role of gluconeogenesis in the hepatic glycogen repletion of diabetic rats. *J. Clin. Invest.* 89:36–45.

19. DeFronzo, R. A., R. C. Bonadonna, and E. Ferrannini. 1992. Pathogenesis of NIDDM. A balanced overview. *Diabetes Care.* 15:318–368.

20. Chiasson, J. L., J. Liljenquist, B. A. Finger, and W. W. Lacy. 1976. Differential sensitivity of glycogenolysis and gluconeogenesis to insulin infusions in dogs. *Diabetes.* 25:283–291.